第 25 回海洋工学シンポジウム　平成 27 年 8 月 6, 7 日The 23rd Ocean Engineering Symposium, August 6-7, 2015
日本海洋工学会・日本船舶海洋工学会ＪＦＯＥＳ　＆　ＪＡＳＮＡＯＥ

OES25-047

Numerical and Experimental Studies on Multiphase Flow in Tsunami with Oil Spill

Wai Phyo KYAW	Department of Naval Architecture and Ocean Engineering, Osaka University E-mail: phyo@naoe.eng.osaka-u.ac.jp
Atsushi YAMADA	Department of Naval Architecture and Ocean Engineering, Osaka University
Youhei TAKAGI	Department of Materials Engineering Science, Osaka University
Hiroyoshi SUZUKI	Department of Naval Architecture and Ocean Engineering, Osaka University
Naomi KATO	Department of Naval Architecture and Ocean Engineering, Osaka University

Abstract

Numerical simulation for oil spill from the oil tanks in the industrial parks and mixing of oil with sediment soil particles from the viewpoint of risk management of Osaka Bay area are urgently needed. The first step to achieve the complete scenario is to deal with the tsunami triggered oil spill. In this research, experiments and simulations were carried out to get deep insight of oil diffusion and movement when subjected to an incoming wave. Simple experiments and visualizations at a laboratory scale were carried out. Then, a numerical method to simulate the whole scenario of these experiments was used. The simulation code includes multiphase (oil-water-air), convection-diffusion effect, and up most three dimensionality. For the future work, after validating the simulation code with the experiments, then the next step is to mix the spilled oil with soil particles shall be carried out in both experiments and simulations.

1. INTRODUCTION

1.1 Background

In 2011 Tohoku earthquake, the tsunami induced run up caused movement of oil tanks and oil spill in Kesennuma Port. A total 11523 kiloliters of oil, mainly heavy oil as well as light oil and gasoline, was estimated to be spilled out due to the drifted oil tanks mostly. According to Kesennuma City, 22 out of 23 tanks (carrying 40 to 3,000 kilolitres) that were in the Minami Kesennuma district were destroyed by the tsunami. This could fill 32 swimming pools with a length of 25 meters. Also, in Ofunato, fuel oil tanks suffered damage and 800 kiloliters of heavy oil spilled out from a cement plant. In both cases, some part of the oil spill was not observed on the sea surface after the disasters.

Kesennuma Bay area was changed into a sea of fire during the Great East Japan Earthquake. At the entrance of the bay, there was a group of heavy oil and gasoline fuel tanks to fuel the fishing boats. When the tsunami inundation hit those oil tanks, most of them broke and drifted into the bay along with spilled oil. This major spillage of heavy oil strengthened the fire. In addition, the debris carried along the wave was soaked in the spilled out heavy oil and acted as a candle wick, and kept up the fire for a long time. At the same time, they were dispersed by the wind and tsunami, and created a great fire which even spread to the isolated island of Oshima. The flame spread along the sea and burned across a large expanse.

1.2 Submarine Oil Spill

If the tsunami strikes the industrial parks which usually include fuel and chemical oil tanks, the inundation usually causes drifting of the tanks, which consequently damages to the pipelines assembly, and in severe case, direct spill from the tanks. The oil spilled out not only has a potential for fire and pollution for the port facilities and inland structures, but also the oil drift together with the back wash of the tsunami into the sea has serious environmental problems. Formerly, the oil spilled into the sea was known to be distributed on the surface and drifted along with the wind, wave and current. Yet, unfortunately, in recent disasters, it was found that oil spill was not only occurred on the surface but also found under the sea surface, a new type of oil pollution which can be referred to as submarine oil pollution.

Unlike ordinary oil spill, tsunami triggered oil spill comes together with the phenomena of mixing oil with sediment soil particles from the sea floor. Tsunami current has strong turbulence, which leads to the formation of high

turbid sea water. When that water comes in contact with the oil spilled out from the fuel tanks along the coast subjected to the tsunami, there is a potential for mixing of the oil and soil particles. As a consequence, the relatively heavier oil-soil particles mixture usually sinks down to the bottom of the sea rather than floating on the sea surface as in case of ordinary oil spill. This leads to severe environmental problems because it is hard to locate and collect the precipitated oil-soil particles mixture on seabed in a relatively wide area and this mixture has a potential for floating up to the surface again due to the consequence of other disasters like storms.

1.3 Analysis of the disaster and countermeasures at coastal industrial zones

There were certain tanks which proved to be resistant to that kind of disaster, comprising both earthquakes and tsunamis. During the Great East Japan Earthquake, tsunami waves of over 7 metres high hit the Sendai Harbour of Miyagino Ward in Sendai City. Two prestressed concrete (PC) structure water supply tanks were totally flooded, and one of them was collided with a container vessel. However, none of them had major damage to its main body.

Prestressed concrete (PC) structure refers to one with concrete wall stressed by piano wires to raise the structural strength as well as resistance, and promote durability. It is usually utilized in the construction of water supply tanks of high capacity to withstand relatively high water pressure. However, in case of fuel tanks, the structure is typically relied on steel plates.

With the adoption of the PC construction method, the fuel tanks destroyed by the tsunami will be reconstructed in Kesennuma City. Eight tanks with a total capacity of 7000 kilolitres will be built in the Minami Kesennuma District by fall 2016. Of course, the tanks with the PC construction have the advantage of the potential resistance to be drifted away by the tsunami of the same scale of the Great East Japan Earthquake, and to allow them to withstand collision from floating debris. However, there exists a chance of bursting out for the pipe connections to cause the oil leakage.

Before the Great East Japan Earthquake, the potential risk of fuel tanks in coastal industrial zones being destroyed by tsunami waves was identified, but virtually, there was no countermeasure for this case. The Fire and Disaster Management Agency analysed the relationship between depth of inundation and extent of damage at fuel tanks in both Iwate and Miyagi Prefectures after the disaster. And it had been found that if the height of the tsunami inundation is between 2.5 to 5 metres, the pipes start to burst, and when the inundation rises above 5 metres, the main body of the tank suffers damage as well.

The tsunami fire of Kesennuma Bay revealed the disaster risks that lay in the coastal industrial zones, where fuel tanks concentrate. Based on the data, they created a simulation model of tsunami damage, and instructed 33 prefectures with petrochemical complexes to review their disaster prevention plans. In this disaster, oil also spilled out even from damaged pipes. The Fire and Disaster Management Agency expanded the subject of their requirement to install emergency shutdown valves, which prevent fuel leakage from the pipes, for tanks with a capacity of over 10 thousand kilolitres to over 1000 kilolitres.

1.4 Risk Management in Osaka Bay Area for Oil Spill

Along the coastal line of Osaka Bay down to Wakayama Prefecture, there is an intensive distribution of energy related infrastructures. In fact, there also is a potential for Nankai Trough earthquake which can bare a seismic intensity of 6 or smaller at Osaka Prefecture and can promote a tsunami with maximum wave height of 6 metres along the coastal line of Osaka Bay. It is urgent to describe the complete scenario of tsunami triggered oil spill from the oil tanks in the industrial parks mixing with oil particles from the viewpoint of risk management of Osaka Bay area.

2. OVERVIEW OF THE DISASTER SCENARIO

The complete scenario of this phenomenon includes various aspects to be considered in; multiphase flow, drifting of oil tanks, mixing of the oil and soil particles. In the current research, as a very beginning step, only the case of multiphase flow for the behavior of oil response to the incoming wave of water is analyzed.

According to what we have seen in the previous Tsunami disasters, the whole scenario for this research can be categorized into 3 phases:

Phase 1:: Tsunami comes to the shore where the industrial parks with oil tanks, breaks the oil conveying facilities, and causes the minor oil spill.

Phase 2:: With enough wave energy, the Tsunami can even break the oil tanks, cause drifting and sloshing of oil tanks, and lead to major oil spill.

Phase 3:: The oil spilled out from the Phase1 and Phase2 mixes with tsunami triggered turbid water, and some portion sinks down to the bottom of the sea.

The current research only dedicates in dealing with Phase 1 and Phase 2 concerns, conducting experiment to analyze the phenomenon of oil response to incoming wave, and using multiphase flow simulation to evaluate the code efficacy to represent the phenomena. Also, as outline above, likewise in case of the Kesennuma City, PC structures will replace steel oil tanks, however, there is a potential that the tanks would be flooded by the inundation of the Tsunami. Hence, a model of oil reservoir which contains oil with the same level of ambient water was used in this research. The oil reservoir was placed at the one end of a 1 metre long tank, while the wave was created from the opposite end. In both experiment and simulations, the wave was created by dam break method to represent the wave close to the tsunami case.

3. EXPERIMENAL SETUP FOR MODELED PHENOMENA

Experiment in the laboratory scale for the oil response behavior after being hit by the wave was carried out in

laboratory of Osaka University. With the help of high speed cameras, the movement of oil was recorded for every split second. The experimental setup is as shown in Fig. 1. When the movable slide wall (green) was lifted up, the water broke as the behavior of a dam breaking phenomenon. This would create a wave which heads towards the oil reservoir.

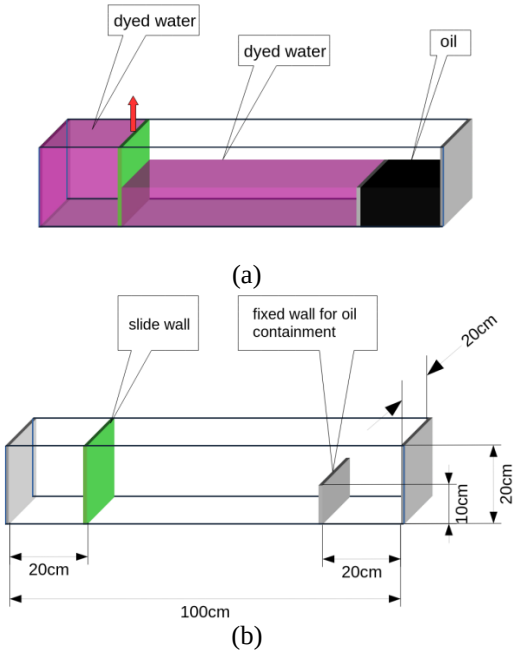

Fig. 1 (a) Sketch of experiment setup (b) Detail dimensions of the tank and wall positions

To achieve the precise time history of the movement of oil after removing the wall, the area closed to the oil reservoir was scaled finely with centimeter mesh. The total volume of water inside the tank was 10000cm^3, and 2000cm^3 of oil, representing the 10% of the volume of water, was kept in the reservoir.

4. COMPUTATIONAL METHODOLOGY AND IMPLEMENTATION TO SOLVE MODELED PHENOMENA

4.1 Multifluid Momentum Equations and Implementation of Drag Models

The simulation was carried out using the same material properties and computational domain of the same size as the experiment. The implementation of the simulation was achieved by the use of OpenFOAM CFD package (version 2.3.1) which provides a collection of libraries and utilities, which can be used to make custom CFD solver for various types of applications. The 'multiphasEulerFoam' solver was used and it is developed by K. E. Wardle and H. G. Weller[1].

The governing equations for the incompressible, isothermal flow for multifluid model was constructed by sets of mass and momentum equations for each phase *k*:

$$\frac{\partial \alpha_k}{\partial t} + \vec{u}_k \cdot \nabla \alpha_k = 0, \tag{1}$$

$$\frac{\partial(\rho_k \alpha_k \vec{u}_k)}{\partial t} + (\rho_k \alpha_k \vec{u}_k \cdot \nabla)\vec{u}_k = -\alpha_k \nabla p + \nabla \cdot (\mu_k \alpha_k \nabla \vec{u}_k) + \rho_k \alpha_k \vec{g} + \vec{F}_{D,k} + \vec{F}_{S,k}, \tag{2}$$

where the suffice k stands for each phase. α_k is the phase fraction of each phase so that the total summation of α_k of all phases is 1; $\alpha_k \le 1$. ρ_k and $\vec{u}_k$ are the density, velocity for each phase, $\vec{g}$ is the acceleration due to gravity. The interface momentum transfer or drag force $\vec{F}_{D,K}$ and the surface tension force $\vec{F}_{S,K}$ are interfacial forces. But for current research, surface tension force was neglected as its contribution was very small as the flow was mainly advection dominant flow. However, the solver itself includes the surface tension capability (based on the continuum surface force model of Brackbill [3]) and surface contact angle effects are also included in the solver.

Hence, the drag force $\vec{F}_{D,K}$ is given by

$$\vec{F}_{D,k} = \frac{3}{4}\rho_c \alpha_c \alpha_d C_D \frac{|\vec{u}_d - \vec{u}_c|(\vec{u}_d - \vec{u}_c)}{d_d}, \tag{3}$$

$$\vec{F}_{D,k} = \alpha_c \alpha_d K(\vec{u}_d - \vec{u}_c), \tag{4}$$

where K is

$$K = \frac{3}{4}\rho_c C_D \frac{|\vec{u}_d - \vec{u}_c|}{d_d}, \tag{5}$$

where the subscripts *c* stands for the continuous phase and *d* for the dispersed phase values.

The drag force is generically calculated inside the solver. A simple advantage in the drag force calculation is just to return the value of *K*. And, also, the value of the drag coefficient C_D, which is dominant in the equation of *K*, is also achieved by the various proposed model. In the literature, a variety models for the deduction of C_D were proposed. Consequently, several common models have been developed in the OpenFOAM. In current case, the popular model of Schiller and Naumann [4] was used. This model considers as C_D a function of the Reynolds number *Re* as shown below:

$$C_D = \begin{cases} \dfrac{24(1 + 0.15Re^{0.683})}{Re}, & Re \le 1000, \\ 0.44, & Re > 1000, \end{cases} \tag{6}$$

where

$$Re = \frac{|\vec{u}_d - \vec{u}_c| d_d}{\nu_c}, \tag{7}$$

where ν is the kinematic viscosity of the continuous phase.

There are two ways to calculate the drag coefficient. The first method is to specify directly a dispersed phase in a continuous phase. The second method is independent calculation where each phase is considered as 'dispersed phase'. In the latter method, the overall drag coefficient for the momentum equations is taken as the volume fraction weighted average of the two values. This scheme is called blended scheme, and useful when solving the flow in the

region in which either phase is primary phase. In current research, only constant droplet diameter size (defined independently for each phase) is assumed while models for variable droplet size can be implemented with this flexible framework.

4.2 Interface Capturing

The interface compression method developed by Weller [5] is used to implement interface sharpening. The comparison of the methods used for interface sharpening and interface reconstruction algorithms for different CFD codes was done by Gopala and van Wachen [6]. This comparison is helpful in conducting trade-off methods between effectiveness and cost.

This scheme of interface compression developed by Weller [5] adds an additional 'artificial' compression term to the left hand side of the volume fraction transport equation for each phase

$$\frac{\partial \alpha_k}{\partial t} + \vec{u}_k \cdot \nabla \alpha_k + \nabla \cdot \left(\vec{u}_c \alpha_k (1-\alpha_k)\right) = 0 . \qquad (8)$$

The value of the artificial interface compression velocity $\vec{u}_c$ is given as

$$\vec{u}_c = \min\left(C_\alpha \vec{u}, \max(\vec{u})\right) \frac{\nabla \alpha}{|\nabla \alpha|}, \qquad (9)$$

where $\vec{u}_c$ is the interface compression velocity to suppress the volume fraction field and keep a sharp interface. To activate this term only in the interface region, the term $\alpha_k(1-\alpha_k)$ is added. And, in addition, $\nabla\alpha/|\nabla\alpha|$ ensures that the direction of the interface compression velocity is always towards the interface to compress against the surface.

Even in the worst case, dispersion of the interface can only occur as the same magnitude as the local velocity, so that the magnitude of velocity $\vec{u}_c$ is used in the interface compression equation. The solver has the option, to switch whether interface compression shall be used or not, by using the coefficient C_α. Although C_α can mathematically be any arbitrary value greater than 0, if one restricts $C_\alpha \leq 1$, equation (9) will reduce to

$$\vec{u}_c = C_\alpha \vec{u} \frac{\nabla \alpha}{|\nabla \alpha|} . \qquad (10)$$

Thus, C_α is considered as a binary coefficient switch which turns interface compression on (1) or off (0). For a given phase pair, when C_α is set to be 0, there will be no imposed interface compression, which means that there is a phase dispersion according to the multifluid model. On the contrary, if C_α is set to be 1, VOF is applied across the interface to achieve interface capturing. In current simulation, C_α is defined and applied independently for all phase pairs in the implementation of the solver. For specific phase pair interface, C_α is set to 1 to keep a sharp interface through out the whole simulation. (.i.e in air-oil and air-water interfaces). And conversely, C_α can be set to 0 for dispersed phase modeling in the other phase pair (water-oil interface) so that there is no interface compression.

Though interface reconstruction methods, for example Piecewise Linear Interface Construction (PLIC) are more accurate than current interface compression method, the development of Weller has the advantage of being easy to implement the solver and relatively faster than others. In addition, the most preferable advantage is that this method is mass conservative [6]. However on the other hand, the current method is not much desirable in small scale surface tension driven flow (capillary rise for the reason of the development of parasitic wavy current at the interface). However, for current case, the flow is mainly advective, and moreover, the undesirable interfacial currents can also be restricted by maintaining the Courant number Cr by means of subtime stepping and restricting C_α = 1.

4.3 Dynamic C_α Switching

As described in the above outline, the interface sharpening and dispersion can be manually controlled by presetting the C_α value. However, it is more convenient if C_α value can alternate dynamically as necessary, as the simulation process marches. This leads to the implementation of an upgraded solver, which enables simulation of complex flow which includes any combination of flow regimes ranging from fully dispersed to fully segregated. The drawback of this implementation is deciding by which method the switching between the dispersion and segregation of the interface form. This is the main controversial work dealt by various researchers who try to couple the multi-fluid and VOF methods. However, according to those outlined above, in this solver implementation, dynamic switching of the interface sharpening can only be occurred in the regions where the flow is segregated through implementation of spatially non uniform C_α field(s). There are also other proposals, and one of which is that this dynamic switching can be set according to predetermined flow regime map [7]. Yet, this approach is merely effective in the flow in simple geometry; however, this current research is dealing with a relatively random nature of flow after the wave striking to the oil reservoir. Hence, current case asks for a more general physic based approach.

From a more general point of view, one of the switching methods is that the sharp interface capturing method should be applied where the droplet size is sufficient enough to be able to be captured the curvature by the local mesh size. On the other hand, when the droplet size is smaller than the local mesh size, the interface capturing method cannot catch the curvature of the droplet and the flow regime in that area is regarded as dispersive flow. This approach will surely need a method to predict the local droplet size (like population balanced method) and comparison of the droplet size with local mesh size to decide switching C_α on (1 VOF) or off (0 multi-fluid).

However, in the current solver implementation, the switching function based on the work by Cerne et al .[2] is used. This switching relies on the magnitude of the gradient of the volume fraction, which assumes that if the gradient of the volume fraction is less than some cutoff value, there is only phase dispersion and the interface sharpening is deactivated. The gradient of volume fraction γ is the normalized magnitude of phase fraction as shown below:

$$\gamma = \frac{\nabla \alpha}{\max(\nabla \alpha)}. \quad (11)$$

Hence, when($\gamma > \gamma^*$) , there is no dispersion (C_α =1), and interface sharpening is activated. Cerne et al. [2] recommended a cutoff value of 0.4: but, γ is the normalized value so the corresponding value may be somewhat different. The downside of this method is that it will apply interface compression to the already sharp interface if γ near that interface is high, and let the interface dispersion where dispersion is already happened if γ is low. Nonetheless it is an acceptable model for the coupling, and has been implemented in the solver.

In this research, two simulations were conducted: one in which dynamic C_α switching is on and other in which C_α values are fixed. In both cases, the entrainment of air into any liquid phases in neglected thus C_α is always 1, keeping a sharp interface for any air-liquid interfaces (interface sharpening is on) during the whole simulations. Conversely, only the C_α setting of liquid-liquid interface is different between these two simulations. In the first simulation, the liquid-liquid phase is dispersed and segregated dynamically, while in the second simulation, the liquid-liquid interface will only be set to interdisperse and sharp interface will not be occurred.

4.4 The Solution Procedure

The procedure of calculation of the Multifluid-VOF coupling hybrid solver is as shown [1].

- Update timestep according to Courant number limit (ratio of timestep to interface transit time in cell)
- Solver coupled set of volume fraction equations with interface sharpening for selected phase pairs ((8) with multiple subtimesteps);
- Compute drag coefficients;
- Construct equation set for phase velocities and solve for preliminary values;
- Solve pressure-velocity coupling according to Pressure Implicit Splitting of Operators (PISO) algorithm:
  - Compute mass fluxes at cell faces;
  - Define and solve pressure equation (repeat multiple times for non-orthogonal mesh corrector steps);
  - Correct fluxes;
  - Correct velocities and apply BCs;
  - Repeat for number of PISO corrector steps;
- Compute turbulence and correct velocities;
- Repeat from 1 for next timestep.

4.5 Numerical Considerations for Stability of Momentum Coupling and Phase Conservation

In maintaining a sharp interface, the velocities on either side of the interface must be equal to match the nonslip interface condition. This is easy in conventional VOF simulation as the phase velocities are equal everywhere in interface since all phases share a single momentum equation. For current method, where a sharp interface is created by the switching on the interface compression terms “on top” of a multifluid formulations, there are specific momentum equations for each phase to be solved, so that an additional virtual drag term is necessary to maintain the velocities at the interface to be equal. Hence, in the implementation of the solver, small residual drag and residual phase fraction constants were added for each phase pair (typically both equal to 1E-03) to stabilize the phase momentum coupling. These residual values were only added to the calculation of drag for momentum coupling stability and therefore did not have any effect on the actual phase fraction or overall phase conservation.

It is necessary to use limiters on the phase fraction and on the sum of the phase fractions before the explicit solution of the phase fraction equation system to ensure the phase conservation for the coupled phase fractions with added interface sharpening. These limiters setting are achieved in a new multiphase implementation of the Multidimensional Universal Limiter with Explicit Solution (MULES) solver framework within OpenFOAM. The MULES algorithm implementation also improves the boundedness of the multiphase VOF-only solver multiphaseInterFoam. The solution of volume fraction transport equation is stabilized by subtimestepping over several subintervals of the overall time step according to Courant number Cr limit. However, for this transient solver, the overall time step is maximized for decreasing the time to solution.

5. RESULT AND DICUSSION

At the end of the experiment, it was found that all the oil inside the reservoir was not spilled out though the reservoir was totally flooded after hitting by the wave. And, in addition, most of the oil was spilled out the reservoir from the portion close to the wall opposite to the incoming wave. But, this portion of oil spilled out may be occurred only in this particular case for this kind of model. However, this phenomenon was very effective to estimate the oil response to the incoming wave.

The results of the simulations proved relative agreement with the experimental outcomes. The critical period of both of experiment and simulations is between **t** (Time) =0.6**s**, the time at which the wave starts to hit the oil reservoir, and **t**=2**s**, when the back wash of the wave returns back. The overall profile snapshots of experiment in this period are shown in Fig. 2. And, the following visual demonstration shows the snapshots comparison of the experiment and two simulations cases: one with dynamic C_α switching (in Fig. 3) and one with fixed preset $C_\alpha = 0$ value in the oil-water phase pair (in Fig. 4). In both simulations, C_α is set to 1 (only VOF is activated) in the air-liquid (air-water and air-oil) phase pairs. Both simulations proved that not all oil was spilled out from the reservoir even though the reservoir was totally flooded. In Fig. 3, it was found that oil dispersion into the water between **t**=1.2s and **t**=2.0s shows a little closer representation to the experiment; unfortunately dispersion was not clearly seen in the experiment, due to oil sticking to transparent wall of the tank.

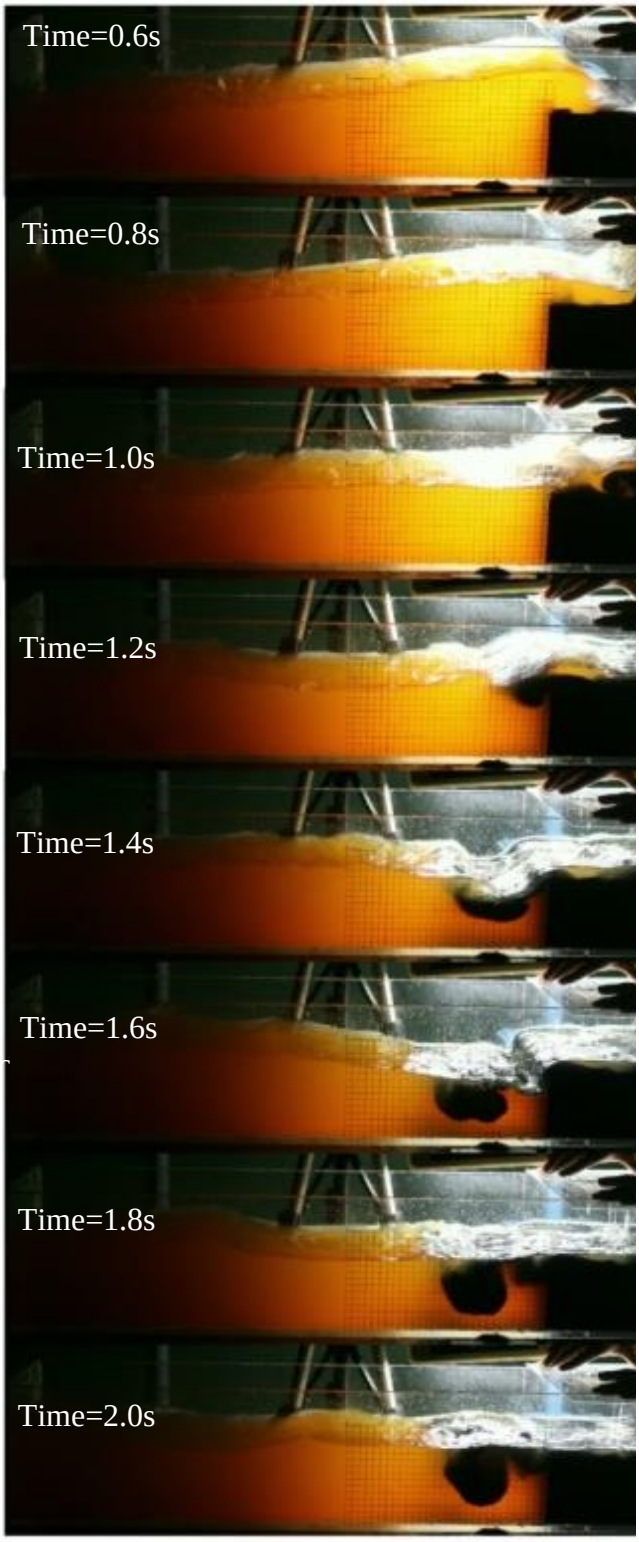

Fig. 2 Profile view of experiment between **t**=0.6**s** and **t**=2.0**s** with emphasizing the detail formation of oil ball phenomenon

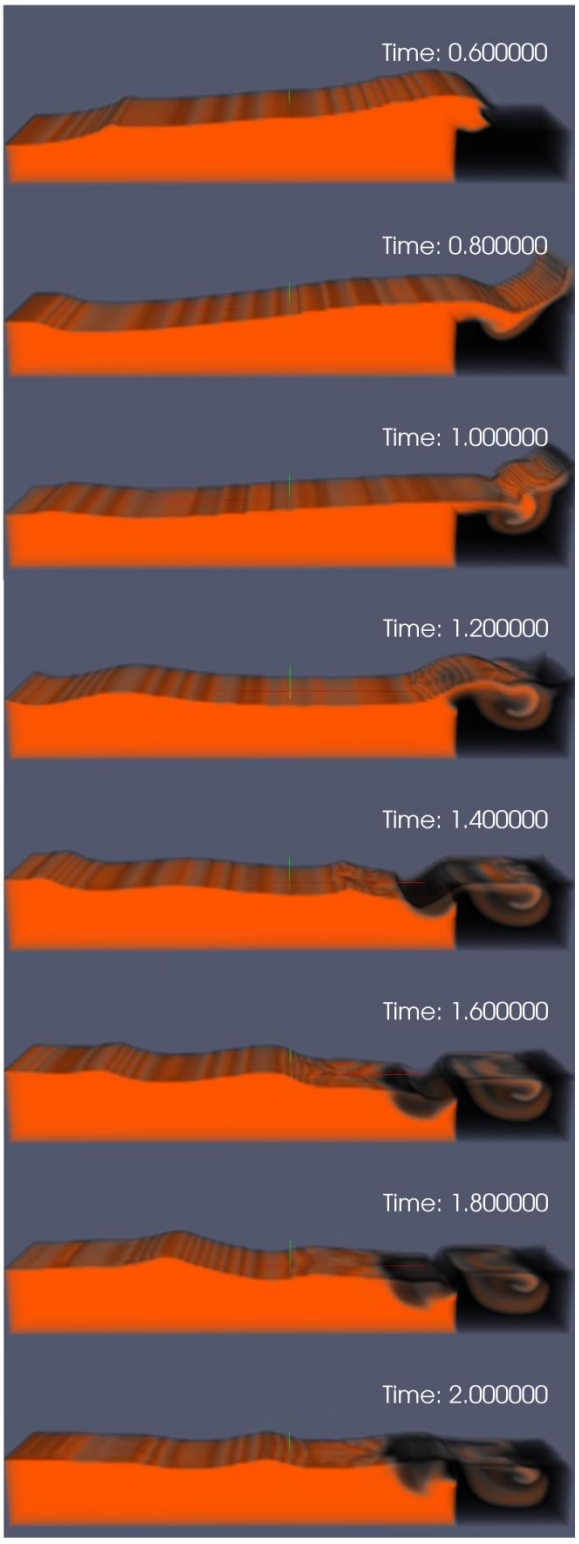

Fig. 3 Profile snapshots of simulation with dynamic C_α switching for oil-water phase pair between **t**=0.6**s** and **t**=2.0**s** with 0.2**s** time step

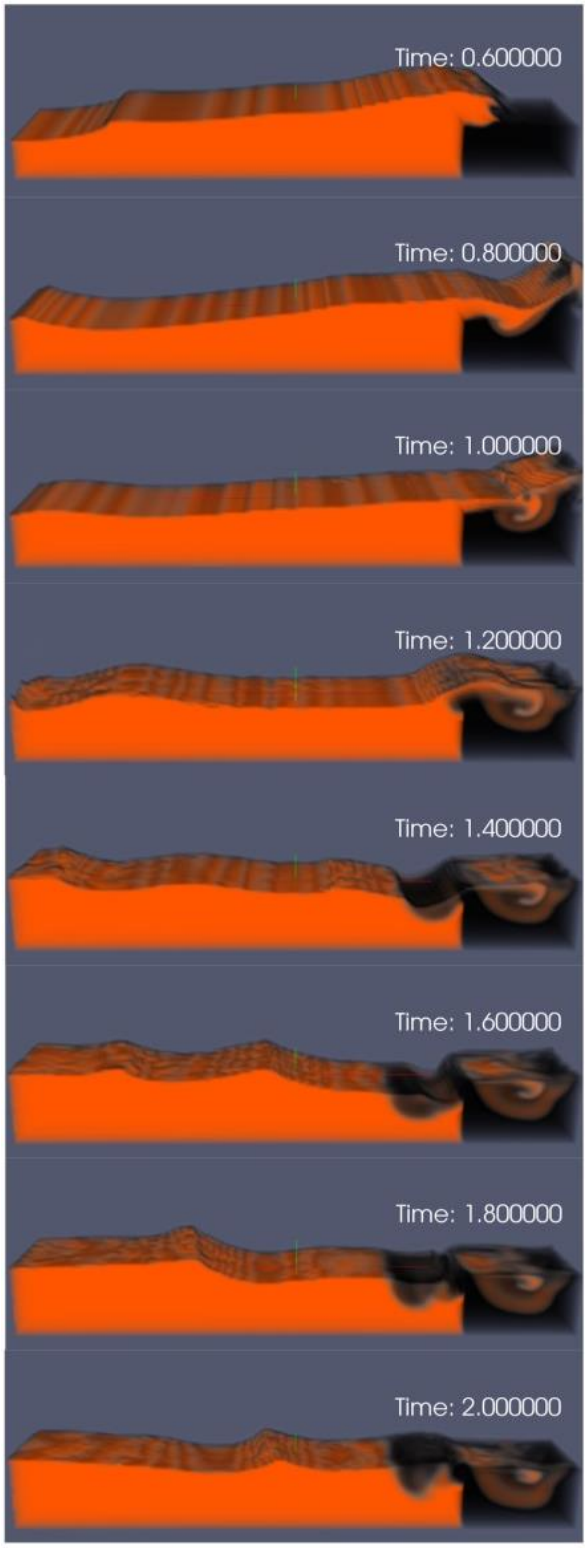

Fig. 4 Profile snapshots of simulation without dynamic C_α switching for oil-water phase pair between **t**=0.6**s** and **t**=2.0**s** with 0.2**s** time step

In addition, the relatively significant oil ball formation phenomenon occurred between **t**=1.4**s** and **t**=2.0**s**. The magnified snapshots of this oil ball formation are reported in Fig. 5. This oil ball is considered to be important for the future research of mixing the oil with the soil particles of turbid water. All the visualization of the results is achieved by the help of post processing tool ParaView (version 4.1).

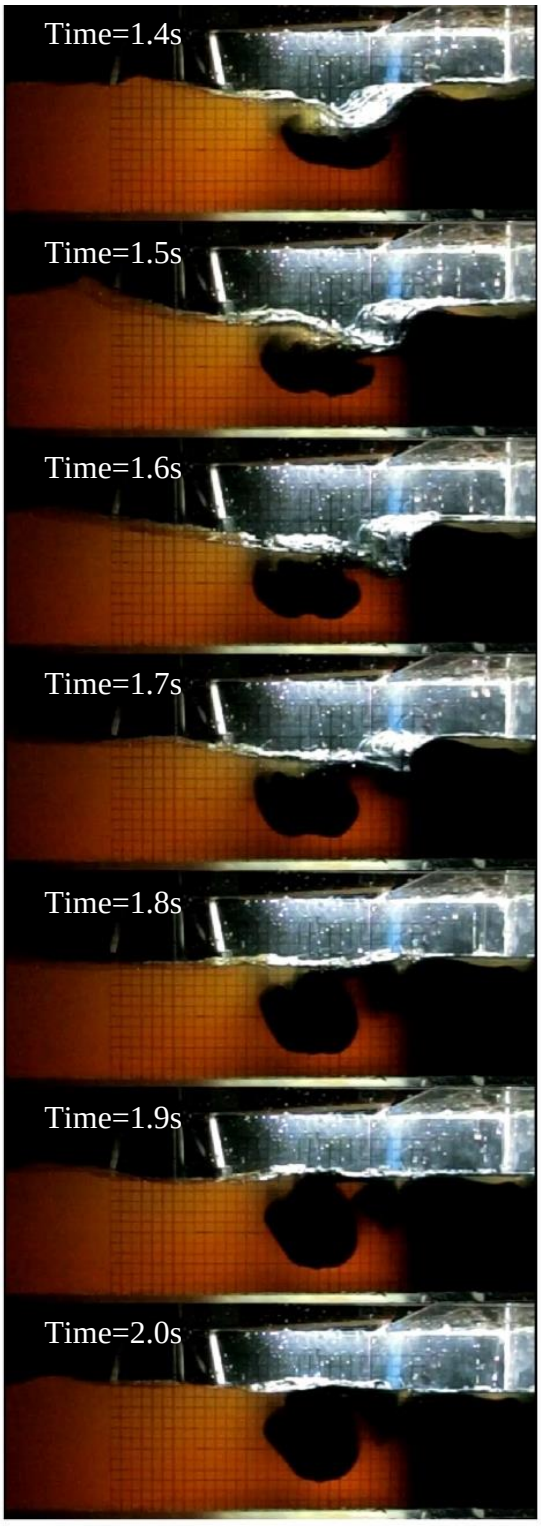

Fig. 5 Emphasizing the detail formation of oil ball phenomenon near the oil reservoir between **t**=1.4**s** and **t**=2.0**s** with 0.1**s** timestep

In the experiment, the maximum depth of the oil ball penetration below the normal water level after flooding was approximately 7.75 cm, and was occurred at **t**=1.8**s**. However, the oil ball in both simulations could merely reach approximately 6cm depth at **t**=1.8**s**. Moreover, the oil ball in experiment showed more segregated in nature than the dispersed oil balls in both experiments.

(a) (b)

Fig. 5 Simulations results of oil ball formation
(a) with dynamic C_α switching for oil-water phase pair
(b) without dynamic C_α switching for oil-water phase pair

6. CONCLUSION

In this research, the phenomenon of oil response to the incoming wave was observed experimentally. This resultant response of oil dispersed and segregated flow in water is simulated in both dynamic C_α swiching (coupled VOF and multifluid) and method fixed C_α=0 value (only multifluid) method. The formation of oil ball after the oil reservoir being hit by the wave was observed, however this phenomenon of oil ball formation appeared weakly in both simulations. Nonetheless, simulation with dynamic C_α switching has a slightly better representation of the phenomenon as the oil dispersion in water is shown a little closer to experiment in the post processing.

7. FUTURE WORK

The multiphaseEulerFoam solver needs to be improved for precise representation of the oil ball formation phenomenon. And the next step to deal with Phase 3 concern, oil mixing soil particles of turbid water shall be carried out experimentally. After the experiment, this phenomenon shall be simulated by coupling the Computational Fluid Dynamics (CFD) and Discrete Element Method (DEM), a code developed by the project of DCS Computing GmbH.

REFERENCES

1) K. E. Wardle and H. G. Weller, “Hybrid Multiphase CFD Solver for Coupled Dispersed/Segregated Flows in Liquid-Liquid Extraction,” Tech. Rep., OpenCFD, 2013
2) G. Cerne, S.Petelin, and I.Tiselj, “Coupling of the interface tracking and thee two-fluid models for the simulation of incompressible two-phase flow,” Journal of Computational Physics, vol.171, no.2, pp.776-804, 2001.
3) I. Brackbill, D. Kothe, and C. Zemach, “A continuum method for modeling surface tension,” Journal of Computational Physics, vol. 100, no.2, pp.335-354, 1992
4) L. Schiller and Z. Nauman, “A drag coefficient correlation,” Zeitschrift des Vereins Deutscher Ingenieure, vol.77, pp. 318, 1935
5) H. G. Weller, “A new approach to VOF-based interface capturing methods for incompressible and compressible flow,” Tech. Rep., OpenCFD, 2008
6) V.R. Gopala and B. G. M. van Wachem, “Volume of fluid methods for immisible-fluid and free-surface flows,” Chemical Engineering Journal, vol. 141. No.1-3, pp. 204-221, 2008
7) L. Strubelj and I. Tiselj, “Two-fluid model with interface sharpening,” International Journal for Numerical Methods in Engineering, vol.85, pp. 575-590, 2011.